

## Shallow Water Table in Arid Urban Zone: Preliminary Study at Sultan Qaboos University Campus, Oman

Marwah Al-Battashi<sup>1</sup>, Ali Al-Maktoumi<sup>1,2</sup>, Anvar Kacimov<sup>1</sup>,  
Ahmed Al-Mayahi<sup>1</sup>, Afrah Al-Shukaili<sup>1</sup>, Said Al-Ismaily<sup>1</sup>, Mohamed Al-Belushi<sup>1</sup>

### مستوى المياه الجوفية الضحلة في المناطق الحضرية الجافة: دراسة أولية في حرم جامعة السلطان قابوس، سلطنة عمان

مروة البطاشي<sup>١</sup>، علي المكتومي<sup>١,٢</sup>، أنفار كاسيموف<sup>١</sup>، أحمد المياحي<sup>١</sup>، أفراح الشكيلي<sup>١</sup>، سعيد الاسماعيل<sup>١</sup>، محمد البلوشي<sup>١</sup>

**ABSTRACT.** A shallow water table (SWT) rises up to several centimeters below the soil surface and even exfiltrates making surface impoundments that are common in humid climates. Recently, SWTs emerged even in arid and semi-arid regions of several metropolitan areas of the Arabian Gulf Cooperation Council (GCC) countries with a pernicious impact on the urban infrastructure, health, ecophysiology of parks and gardens, among others. Quantifying SWT's dynamics and understanding the associated phenomena of water motion and solute transport are vital for finding the proper mitigation techniques and reducing the risks associated with SWT. In this preliminary study, SWT was delineated, its seasonal dynamics was monitored, evaporation losses were quantified, and groundwater chemistry was measured at Sultan Qaboos University (SQU) campus (Oman). The study sites were near the building of the College of Nursing (Wadi N, 4 soil excavations thereafter indicated as S1, S2, S3 and S4) and near the SQU Mosque (Wadi M, 3 locations were labeled 1,2 and 3). Field measurements of SWT in soil excavations, laboratory analysis of collected groundwater samples, and numerical simulation of evaporation using HYDRUS-1D were conducted. The results showed that the water table depth in all excavations in Wadi N increased during June compared to January-March by 24 times (from 0-6 cm to 130-145 cm), while the water salinity increased by 50% (from 4,563 mg/L to 9,164 mg/L). Unlike Wadi N, the water table in Wadi M remained steady (within 4.5-6 cm), while the water salinity of the locations 1 and 2 increased by nearly 40% to 22% (7,948-13,632 mg/L and 7,372-9,075 mg/L), respectively, whereas it decreased by nearly 30% in location 3 (from 9,177 to 6,374 mg/L). These variations in water chemistry suggest that the studied SWT is patchy and caps perched aquifers, which are likely to be disconnected hydraulically from each other and the regional aquifer located at the depth of about 15 m under the local ground surface. Considering the seasonal variation in weather conditions, the results of HYDRUS-1D simulations showed that the evaporation rate in June was higher by about 50% than that for January-March. The discharge from the water table due to evaporation from the whole area of Wadi N was estimated by the model to be around 6600 m<sup>3</sup>. Further studies should determine the source of groundwater that would make possible a hydrological balance for perched aquifers. This would drilling and installing nested piezometers with regular record of SWT and regional groundwater, geophysical surveys of the subsurface, detailed analysis of soil pedogenesis and morphology of the vadose zone, isotope analysis of groundwater, and detailed numerical simulations of groundwater and soil moisture motion.

**KEYWORDS:** Shallow water table; HYDRUS-1D; Aquisalids, Arid regions; Urban groundwater; Waterlogging; Salinity; Evaporation; Sultan Qaboos University; GCC countries

**الملخص:** إن ارتفاع منسوب المياه الجوفية الضحلة إلى عدة سنتيمترات تحت سطح التربة وصولاً إلى تدفقها إلى السطح مكونة مياة سطحية شائعة في المناخات الرطبة. ولكن في الآونة الأخيرة ظهرت مشكلة ارتفاع منسوب المياه الضحلة في المناطق القاحلة وشبه القاحلة في عدد من المدن الحضرية في دول مجلس التعاون الخليجي مخلفةً أضراراً على البنية التحتية والمنشآت، والصحة، والهيدرولوجيا البيئية للمتزهات والحدائق مسببة العديد من الآثار السلبية الأخرى. وبالتالي يعد قياس ديناميكيات مستوى المياه الضحلة وفهم الظواهر المرتبطة بحركة الماء ونقل المواد المذابة أمراً مهماً لإيجاد التقنيات المناسبة للتقليل من المخاطر المرتبطة بمشكلة ارتفاع منسوب هذه المياه. في هذه الدراسة الأولية تم تحديد منسوب المياه الجوفية الضحلة، ورصد ديناميكياتها الموسمية، وقياس مستويات التبخر، ودراسة كيمياء المياه الجوفية بجامعة السلطان قابوس (سلطنة عمان). وشملت الدراسة موقعين أساسيين وهما الوادي القريب من كلية التمريض (تم حفر أربع حفر شُئمت بالترتيب S1, S2, S3, S4) والوادي القريب من مسجد جامعة السلطان قابوس (تضمن ثلاثة مواقع شُئمت بالترتيب L1, L2, L3). وقد تم إجراء قياسات ميدانية للمياه الضحلة في تلك الحفر ومواقع الدراسة وإجراء التحليل المختبري لعينات المياه الضحلة التي تم جمعها. كما تم القيام بالنمذجة العددية للتبخر باستخدام برنامج HYDRUS-1D. وأظهرت النتائج أن عمق المياه الجوفية في جميع الحفر في الوادي القريب من كلية التمريض زاد خلال شهر يونيو مقارنة بشهر يناير - مارس بمقدار ٢٤ مرة (من 0-6 سم إلى 130-145 سم)، بينما زادت ملوحة المياه بنسبة 50% (من 4563 ملليجرام / لتر إلى 9164 ملليجرام / لتر). بينما ظل منسوب المياه في الوادي القريب من المسجد ثابتاً نسبياً (في حدود 4.5-6 سم). كما زادت ملوحة المياه في الموقعين L1 و L2 بحوالي 22% إلى 40% (ملليجرام/لتر 7,948-13,632 و 7,372-9,075 ملليجرام/ لتر)، على التوالي، بينما انخفضت الملوحة بنسبة 30% تقريباً في الموقع L3 (من 9177 إلى 6374 ملليجرام / لتر). تشير هذه الاختلافات في كيمياء المياه إلى أن المياه الضحلة عبارة عن أحواض متفرقة في عدد من الطبقات الجوفية، والتي من المحتمل أنها غير متصلة هيدروليكيًا ببعضها البعض وكذلك منفصلة عن الخزان الجوفي الرئيسي بالمنطقة الموجود على عمق حوالي ١٥ مترًا تحت سطح الأرض. بالنظر إلى التغيرات الجوية الموسمية، أظهرت نتائج النمذجة العددية أن معدل التبخر في يونيو كان أعلى بنحو 50% من مثيله في الفترة من يناير إلى مارس. بالإضافة إلى أن مقدار التبخر من منسوب المياه الضحلة (الجوفية) من منطقة الوادي القريب من كلية التمريض بأكملها حوالي 6600 متر مكعب تقريباً. نقترح أن تتضمن الدراسات المستقبلية آليات لتحديد مصدر المياه الجوفية التي من شأنها أن تجعل التوازن الهيدرولوجي ممكنًا لخزانات المياه الجوفية. هذا من شأنه يتطلب حفر وتركيب مقاييس ضغط متداخلة مع مراقبة منتظمة لمنسوب المياه الجوفية الرئيسية، والمسوحات الجيوفيزيائية تحت السطح، والتحليل التفصيلي لتكوين التربة وخصائصها، وتحليل النظائر للمياه الجوفية، والمحاكاة العددية لديناميكيات المياه الجوفية وحركة المياه في التربة.

**الكلمات المفتاحية:** منسوب المياه الضحلة، هايدرول، 1D، التربة الرطبة التملحة، البيئات الجافة، المياه الجوفية الحضرية، التشبع بالمياه، الملوحة، التبخر، جامعة السلطان قابوس، دول الخليج العربي.

Ali Al-Maktoumi<sup>1,2</sup> (✉) ali4530@squ.edu.om, Department of Soils, Water and Agricultural Engineering, Sultan Qaboos University, PO Box 34, Al-Khoud 123, Sultanate of Oman, Water Research Center, Sultan Qaboos University, Sultanate of Oman.



## Introduction

**W**ater table rise (WTR) brings groundwater from the depth of several meters to several centimeters from the soil surface. Moreover, shallow water table (SWT) and WTR can even fill in topographic depressions and basements of the buildings and construction sites. Surprisingly, even in hyperarid climates of the Arabia, SWT and WTR are observed in certain urban districts (Abu-Rizaiza et al., 1989; Abu-Rizaiza, 1999; Al-Senafy et al., 2015; Bob et al., 2016).

Waterlogging by SWT is often attributed to the exponential growth of population and it is associated with the accelerated expansion of urban areas in developing countries (i.e. having a high flow of wastewater and lack of a proper sewer system). Another cause is the leakage from the water distribution network. WTR becomes a serious issue, especially, when municipalities have no effective integrated programs for inspecting the buried water mains and operating-maintaining the water networks. Disturbance of the natural drainage systems is also reported as one of the main reasons WTR in urban settings (Abu-Rizaiza et al., 1989; Abu-Rizaiza, 1999). This occurs when foundations of residences, commercial buildings, and other engineered infrastructures are placed within the streams or in the floodplain of the wadis. Consequently, during the rain, water cannot drain naturally, as before urbanization, but rather tends to accumulate near the ground surface forming “perched aquifer systems”. Urbanization causes compaction and vertical heterogenization of the porous substrate (soil and rock) on which infrastructure is based (Kacimov et al., 2021). Moreover, an increased recharge derived from excessive irrigation of urban parks and gardens (municipal and individual) increases the groundwater level. Irrigation may cause mounding of groundwater hoisted to the ground surface, especially when a shallow impervious layer exists under the topsoil (Abderrahman et al., 2000). Agricultural transformation activities and shifting of plants in cities e.g. removal of native plants and clearing of deep-rooted perennial trees (e.g. Ghaf or Sidr trees) may also cause water tables to rise (Eberbach, 2003). There are also some natural causes, which may contribute to WTR, e.g. hydrogeological and hydraulic characteristics of the subsurface. For example, shallow alluvial aquifers with their recharge zones in the nearby mountains (alluvial fans) may have bedrocks tilted towards the urban areas. Such aquifers can rapidly convey groundwater towards topographically flatter urban areas where this water decelerates in its motion and dissolves more minerals. Unexpectedly, intensive rain periods associated with flash floods in the region (Abu-Rizaiza et al., 1989; Abu-Rizaiza, 1999; Al-Senafy et al., 2015).

WTR has affected many urban areas in the GCC countries, resulting in a wide range of problems depending upon the geotechnical and hydrological conditions, and the construction practices at the sites under con-

sideration (Abu-Rizaiza et al., 1989; Abu-Rizaiza, 1999; Al-Senafy et al., 2015; Allocca et al., 2016). WTR impacts the infrastructure by reducing the bearing capacity of the soil. Capillarity moves water from the ground to the soil surface and concrete of the footing of the buildings (the so-called damping phenomenon) and roads. Upon drying, water evaporates and the salts left behind crystallize within the pores of the masonry units. The salt crystals dissolve during humid periods and recrystallize upon subsequent drying. Hence, repeated cycles of wetting and drying eventually cause corrosion, cracking and disintegration in the steel and walls of the buildings. Asphaltic streets could be damaged because of the presence and ingress of water in the pavement structure (Saeed et al., 2019). Water pipes and electrical cables can be deteriorated due to the polluted or high salinity shallow groundwater (Abu-Rizaiza et al., 1989). The occurrence of SWT can also form small lakes (ponds) which are a good environment for breeding and spreading insects like mosquitoes, flies, and roaches. Consequently, this can spread water-borne diseases from ponded water and cause nauseating smells and unsafe driving conditions (Abu-Rizaiza et al., 1989; Sharp, 2010). All of these may cause treacherous impacts on the life cycle of the cities’ geotechnical systems and cause financial losses to the building owners and municipalities that affect the economy because all structural damages need regular reparation and sanitary treatment for the diseases (Abu-Rizaiza et al., 1989; Abu-Rizaiza, 1999; Al-Sefry and Şen, 2006; Al Senafy, 2011; Al-Senafy et al., 2015; Raymond et al., 2020).

WTR in urban areas in Oman may increase the severity of the risks mentioned above, so it is necessary to understand the causes and effects in order to propose solutions that limit the development of this problem in the future. Groundwater under SWT can be pumped out. A monitoring system to detect any leakage from the water networks and surface storage should be deployed in areas prone to WTR. Additionally, the irrigation efficiency of ornamental plants and urban crop-cultivation under urban gardening and agriculture need to be improved to reduce the volume of the irrigation return to underlying shallow aquifers (Al-Mayahi et al., 2019; Rufí-Salís et al., 2020). Designing and implementing a dewatering operation requires consideration of the geo-mechanical properties of the soil and the potential impact of any dewatering technique on the buildings’ foundations within the affected area. A proper mitigation system as the placement of the dewatering and observations wells, which control and predict groundwater fluctuations in response to pumping and monitor the seasonal variations of the recharge, should be planned (Abu-Rizaiza, 1999; Al-Sefry and Şen, 2006; Al Senafy, 2011; Morway et al., 2013; Al-Senafy et al., 2015).

There are several numerical codes used in simulating water dynamics in porous media, particularly with WTR. For example, HYDRUS simulates the flow and transport

of water in the vadose zone. HYDRUS software can also be used to model evaporation, infiltration, salt, and heat fluxes in the vadose zone (Šimůnek and van Genuchten, 1999; Šimůnek et al., 2016; Radcliffe and Šimůnek, 2018). This study explores WTR at the Sultan Qaboos University (SQU) campus, Oman. The field investigations and soil observations, laboratory analysis, and preliminary numerical modeling are reported in this work.

In Figure 1, variable  $a$  designates the depth of the water table. SWT in the lake of Figure 1 above had  $a$  of about 15 cm. That was a great surprise because the regional water table monitored by the the Ministry of Agriculture and Fisheries Wealth and Water Resources (MAFWWR) in the nearby monitoring wells was about  $a=15$  m (Figure 1a). By 2019, the campus had no observational wells/piezometers. Only few occasional deep drillings and excavations went to the depth of  $b= 5-10$  m deep (during construction of new SQU buildings). SWT was detected at the depths of about  $a=2$  m. At SQU, there was no conceptual model of the shallow subsurface pore water. The status of this water was not clear because the vadose zone (Figure 1a) was presumed to be 15 m thick and the topsoil was considered to be dry enough to sustain all on-campus constructions. The tacit assumption considered all water infiltrated from the SQU sources (primarily, irrigation of huge green zones of ornamental vegetation) percolates easily and rapidly to the regional aquifer. Since discovering a surprising SWT and thin vadose zone, SQU mobilized our team to explore the phenomenon. Several monitoring pits having the depth of  $b=1-4$  meters (Figure 1a and b) were excavated. The loci of these pits were selected with numerous restrictions: most of the campus area is paved, covered by parks-lawns and infrastructural objects (see Figure 1a). Unfortunately, even some remaining bare soil areas at the campus could not be excavated because of electricity-internet cables, which are buried there. Also there are many buried pipes of sewage and fresh water network.

For the hydrological balance of the campus area during 2019-2021, the known inputs were:

a) Good records of meteorological data from the SQU and another weather station. In particular, these data showed no serious rains between March 2020 and April 2021. Therefore, there was no detected runoff in the below studied wadies. Also, the data on irrigation of the campus green zones were available and excess irrigation, potentially contributing to WTR on campus, could be roughly assessed. The recent national (Oman) statistics reports that about 25 % of fresh water is lost due to breaches in the subsurface mains and water supply network. It is unclear whether the same quantity of water leaks from the SQU subsurface pipes. The leaks from the subsurface sewage network have also not been measured or assessed.

b) The groundwater level in constructed excavations was monitored for one year. More pits were exca-

vated and groundwater level and water chemistry were measured there.

c) Since 2012, MAFWWR started exploration of the subsurface in a conterminous area (see Fig. 1 b), few tens of meter of the SQU campus. The Al-Jafnin dam will be constructed there. From the Ministry drilling-trenching data, SWT records showed that  $a=2-5$  m that confirmed the hypothesis of patchy, hydraulically disconnected perched aquifers.

It was clear from November 2019 that the key question about the source of the revealed SWT can not be answered by monitoring the excavations, measurements of salinity pH and chemistry of unearthed groundwater and seemingly simplistic 1-D modeling of evaporation or infiltration through a shallow ( $a=10$  cm-4 m, Figure 1a) vadose zone. The 3-year program was formulated to conceptualize the subsurface hydrology of the detected perched aquifers. In particular, it was found that loose sediments -soil in all 2019-2020 excavated pits were underlain by a "hard pan" (caliche). The thickness  $c$  (Figure 1 a) of this caliche was several tens of cm. For the whole study area the value of  $c$  is unknown (we indicated this by a question mark in Figure 1a). Water table between the hard pan and regional was not known. In particular, we did not know whether groundwater from the perched aquifers seeps down through the hard pan. Moreover, it was not clear whether the hard pan was horizontal, tilted or undulated (see Figure 1 a), potentially having a variable thickness  $d$ . Therefore, the storage of the perched aquifers shaded in blue in Figure 1b depends on the saturated thickness of groundwater. This storage, in meteorological conditions showed no precipitation and no runoff during the study period (March 2020-April 2021). It was depended on evaporation-transpiration and still-unknown potential seepage downwards (through the hard pan). Indeed the instantaneous storage of unconfined (in particular, perched) aquifers was the difference between the fixed depth of the "bedrock" (or aquitard) and the dynamic SWT. If the caliche layer in Fig 1a was not horizontal or did not make a regular inclined aquifer but has "troughs", like the one shown in Figure 1a, then perched shallow groundwater did move horizontally but stays in such troughs, with an ensued increase of salinity due to evapotranspiration. A long residence time of groundwater in contact with soluble minerals also increased salinity. On another hand, the caliche layer may have "gaps" or "windows" (not shown in Figure 1a) through which groundwater from a perched aquifer above may be funneled to the regional aquifer. That may explain the lack of hydraulic contact between the blue perched aquifers in Figure 1b. Mapping of the hard pan versus SWT was planned for the future. That will require making a relatively dense network of nested piezometers over the campus area. In the above described context of the current uncertainty-

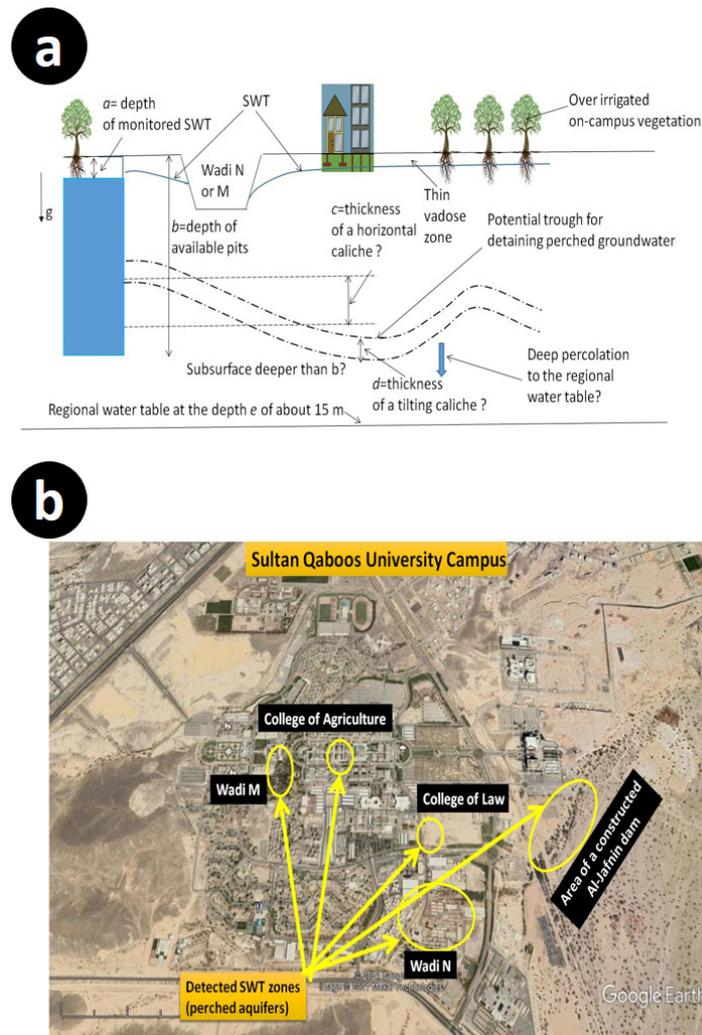


**Figure 1.** Sketch of our current understanding of the status of the shallow perched aquifers in 2021. (a) depicts a vertical cross-section of a perched aquifer; (b) gives an aerial view of the SQU campus with indications of detected patchy perched aquifers.

ties and limitations with the available data, this paper did not aim to give a comprehensive hydrological model of the subsurface at the SQU campus. Our work was rather a preliminary study of the recently discovered perched aquifers. Our motivation stems from direct instructions from SQU higher administration.

## Methodology

The study involved field measurements and laboratory analysis along with numerical modeling using HYDRUS-1D. The following subsections present more details.

### Field Measurements

The field study was carried out at two sites within the campus of SQU: the area behind the College of Nursing, hereafter called Wadi N site (coordinates 23°34'54" N, 58°10'24" E) and the Wadi near the SQU Mosque, hereafter called Wadi M site (coordinates 23° 35'13" N, 58° 09'

46" E) (Figure 2 a, b). The average measured width and length of wadi N were 21.75 m and 595 m, respectively (the area of wadi bed= 12941 m<sup>2</sup>). For wadi M, these sizes were 6.13 m and 490 m, respectively (the area of wadi bed= 3003 m<sup>2</sup>). At these two locations, shallow groundwater was observed. The selected sites were monitored on a weekly basis. Water depth from the ground surface was measured in four different places distributed along Wadi N (Figure 2c, Table 1) and three locations from Wadi M (Figure 2d, Table 1).

### Laboratory Analysis and Weather Data

Water samples from the studied locations of wadies M and N were collected for laboratory analysis of total dissolved solids (mg/L). Soil samples were also collected for the analysis of soil texture, soil salinity (ECe), soil moisture, and bulk density following the standard procedure by Soil Survey Staff (2014). During the study period, weather data including air temperature, relative humid-

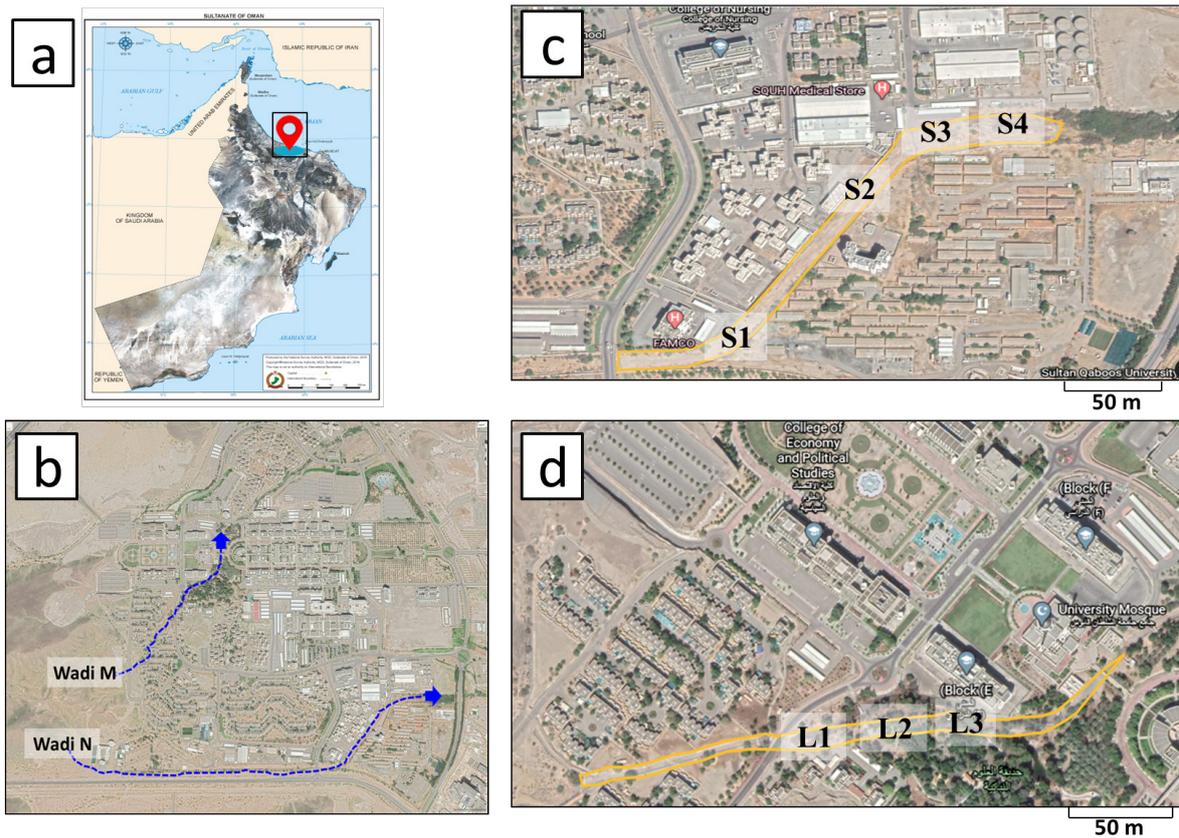


**Figure 2.** Map and locations of the study area. a) Map of Oman, b) Google earth image showing the study areas along the two wadis, c) Google earth image showing Wadi N with measurement locations, d) Google earth image showing Wadi M with measurement locations.

ity, precipitation, solar radiation, and wind speed (Figure 5 a,b,c,d) were collected daily from a weather station at the Agricultural Experiment Station (AES) in SQU located within 1 km from the study site (23°35'54.06", 58°09'48.96"E). Hence, the used meteorological data are representative for both wadis. The weather station was at an elevation (z) of 52 m above the mean sea level. The collected meteorological data were used to calculate the reference evapotranspiration (ET<sub>o</sub>) using the FAO Penman-Monteith method, following the guideline set by Zotarelli et al. (2010). This ET<sub>o</sub> is found to be 4.37 mm/day.

**Table 1.** GPS coordinates for measurements locations in Wadi N and Wadi M

Wadies	Locations	Coordinates	
		N	E
Wadi N	S1	23°34'57.62"	58°10'18.43"
	S2	23°35'4.76"	58°10'23.91"
	S3	23°35'6.71"	58°10'29.03"
	S4	23°35'6.81"	58°10'29.56"
Wadi M	L1	23°35'19.40"	58° 9'49.62"
	L2	23°35'21.74"	58° 9'50.49"
	L3	23°35'23.97"	58° 9'54.49"

### Numerical Modeling

The soil excavation S3 (presented as measurement location S3 in Wadi N, see Figure 2 C) was selected for modeling of evaporation from the water table using HYDRUS-1D (Šimůnek et al., 2016). The simulation was done for two scenarios. The first scenario modeled the period 31<sup>st</sup> -January to 5<sup>th</sup> -March. The depth of the modeled soil profile for this scenario was 38 cm and the number of soil materials (layers) was 4 (Figure 3). The length of the simulation time and the time interval were set for 35 days and 1 day, respectively. In HYDRUS code, the maximum number of iterations was 10 and the water content tolerance was 0.001. The van Genuchten-Mualem (VG-M) (1980) soil hydraulic model was selected with no hysteresis effects. Rosetta package of HYDRUS code was used to predict the VG-M parameters of the soil for each layer using the percentage of sand, silt and clay, and the bulk density (Table 2). The upper boundary condition was set as atmospheric using the reference evapotranspiration data (Figure 5 e). The lower boundary condition (water table) was set as a constant pressure head with a value of 0 cm. The initial condition was in the pressure head, distributed hydrostatically with values of -1000 cm and 0 cm, for the up-

per and lower boundaries, respectively. The profile was discretized into 380 nodes. The second scenario was for modeling the period 1<sup>st</sup> to 28<sup>th</sup> June. The modeled profile depth for this scenario was 60 cm and the number of soil materials was 6 (Figure 3).

The total simulation time was set for 28 days and the time interval was set for 1 day. The discretization of the soil profile was 600 nodes. Set up of iteration criteria, soil hydraulic model, and boundary and initial conditions were similar to the first scenario. The evaporation rate was obtained from the HYDRUS-1D output results of each scenario. The total volume of evaporated water from the entire area of Wadi N was calculated by multiplying the difference in average evaporation rate between the two scenarios times the number of days (31<sup>st</sup>-January to 28<sup>th</sup> -June) times the area of Wadi N.

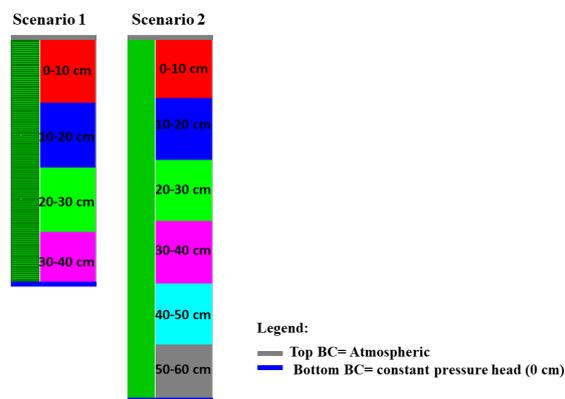


**Figure 3.** Geometry of the modeled soil profile (S3 excavation, Wadi N) for the scenarios 1 and 2. BC is boundary condition.

## Results and Discussion

### Field Observation and Measurement of WTR and Salinity

Wadi N: Figure 4 presents field measurements: water level (cm) and salinity of water (mg/L). For observation points along Wadi N, the water level is presented in Figure 4a. The graphs show a decreasing trend of water level at all observation points. It is worth mentioning that no rainfall events were recorded February to the end of June 2020. Considering the period from 30<sup>th</sup>-January to 5<sup>th</sup>-March, water levels at S1 and S2 were almost constant (130 cm and 0 cm from the ground surface, respectively). Water levels at sites S3 and S4 were nearly at the surface. The water levels of the latter two sites dropped on the 13<sup>th</sup>-February and remained stable till 5<sup>th</sup>-March at 39 cm and 8 cm, respectively. This is because a construction company erected a small bridge and pumped out a large volume of water from the site close to S3 and S4. Hence the developed groundwater drawdown is reflected in the measurements of the water level at S3 and S4 sites. After 3 months (end of June 2020), the water level in all excavations showed a decreasing trend with the depths ranging between 10 to 140 cm. This could be attributed to high average air temperature (37.6 °C; Figure 5a) and low relative humidity (41% on average; Figure 5b) that enhances losses of water via high evaporation. Moreover, the differences water levels among the different locations of wadi N maybe due to the hummocky topographic landscape, or to the effect of low-permeable subsurface soil lenses of caliche that we have observed during our field survey. At the monitoring point of S3 in Wadi N, the measured salinity level was found to be constant at 4,600 mg/L for the period 30<sup>th</sup>-January to 27<sup>th</sup>-February. Measurements on 28<sup>th</sup> of June 2020 indicated a dramatic increase in the salinity level by almost 100% (reaching 9,164 mg/L) (Figure 4b). This increase in

**Table 2.** Soil properties for S3 excavation, Wadi N:  $\theta_r$  and  $\theta_s$  are the residual and saturated water contents, respectively;  $\alpha$  and  $n$  are the VG-M parameters; and  $K_s$  and  $L$  ( $L=0.5$  for all soil types) denote the saturated hydraulic conductivity and HYDRUS pore connectivity parameter, respectively

Depth (cm)	Soil type	Soil particles (%)			Bulk density ( $\text{g cm}^{-3}$ )	$EC_e$ (dS $\text{m}^{-1}$ )	$\theta_r$ ( $\text{cm}^3 \text{cm}^{-3}$ )	$\theta_s$ ( $\text{cm}^3 \text{cm}^{-3}$ )	$\alpha$ ( $\text{cm}^{-1}$ )	$n$ (-)	$K_s$ ( $\text{cm day}^{-1}$ )
		Sand	Silt	Clay							
0-10	Sandy	93.04	6.28	0.68	1.37	24.8	0.0479	0.4219	0.0382	3.0069	774.59
10-20	Sandy	89.03	10.32	0.65	1.12	31.0	0.0418	0.4934	0.0529	1.898	564.05
20-30	Sandy	91.10	6.25	2.66	1.21	18.3	0.0478	0.4726	0.044	2.2262	611.21
30-40	Loamy Sand	86.39	8.78	4.83	1.34	13.1	0.0476	0.4344	0.039	2.0568	323.84
40-50	Loamy Sand	86.49	8.64	4.87	1.44	11.5	0.0478	0.4061	0.037	2.1939	272.43
50-60	Loamy Sand	84.37	10.79	4.85	1.61	21.9	0.0436	0.3554	0.0398	2.0241	132.97

salinity is probably due to intensive evaporation which concentrates salts in the remaining water volume. Furthermore, electricity cables in trenches were submerged in the water (Figure 6a) which can pose a potential risk for people who walk around the area especially if the insulation cover of the cables is peeled off. Patches of crystalized salt stains were also observed in the soil surface near S3 excavation. The patches had fine textured soil which may act as a siphon through which excessive evaporation happens and hence leaving behind more salts to precipitate on the soil surface (Figure 6b). Furthermore, damping, cracking, and disintegration in the walls of the SQU buildings were also observed (Figure 6c). At the end of June 2020, the soil surface near S2 looked almost dry (Figure 7a), whereas it completely dried up at S1 (Figure 7b). The soil surface near S3 and S4 excavations looked moist with some salt accumulation (Figure 7c). It is very likely that as more water evaporates, salts will crystallize on the soil surface and across the drained soil layers.

Wadi M: The water levels in Wadi M show a decreasing pattern from the 10<sup>th</sup> of February to 2<sup>nd</sup> of March 2020 along the observed Wadi section (Figure 4c). In Wadi M, there were no excavations; but the water table was accumulating above the ground level (i.e. above the

wadi bed). The depth of the ponded water was small for point L1 (about 2 cm) but reached 5.5 cm at point L3 downstream of point L1 (about 216.6 m apart). During the study period, 10<sup>th</sup> February to 28<sup>th</sup> June, the water level above the surface in L1 remained constant (ranged from 2.5 cm to 2 cm). Unlike L1, the water level at L2 and L3 increased, reaching 5.5 cm and 6 cm, respectively (nearly doubled). Moreover, it was noticed that the ponding pattern was sporadic along Wadi M as the water table was at the surface at certain zones in the Wadi and disappeared over the other parts of it (Figure 8a and Figure 9a, b). This could be attributed to the undulating wadi bed where the water table appears in low laying portions. Detailed measurements of the change in the wadi bed topography are needed along with digging or drilling a number of observation boreholes along the banks and in the bed of the wadi. This will enrich us in understanding the hydrology of the site, and the direction of seepage in the area.

Contrary to Wadi N, the salinity of the ponded water in all the measured locations at Wadi M decreased for the period extending from 10<sup>th</sup> of February to the 2<sup>nd</sup> of March 2020 (Figure 4d). During the same period, L3 has the highest salinity (ranging between 9,200 mg/L to 8,600 mg/L) as compared to L1 and L2 which had almost

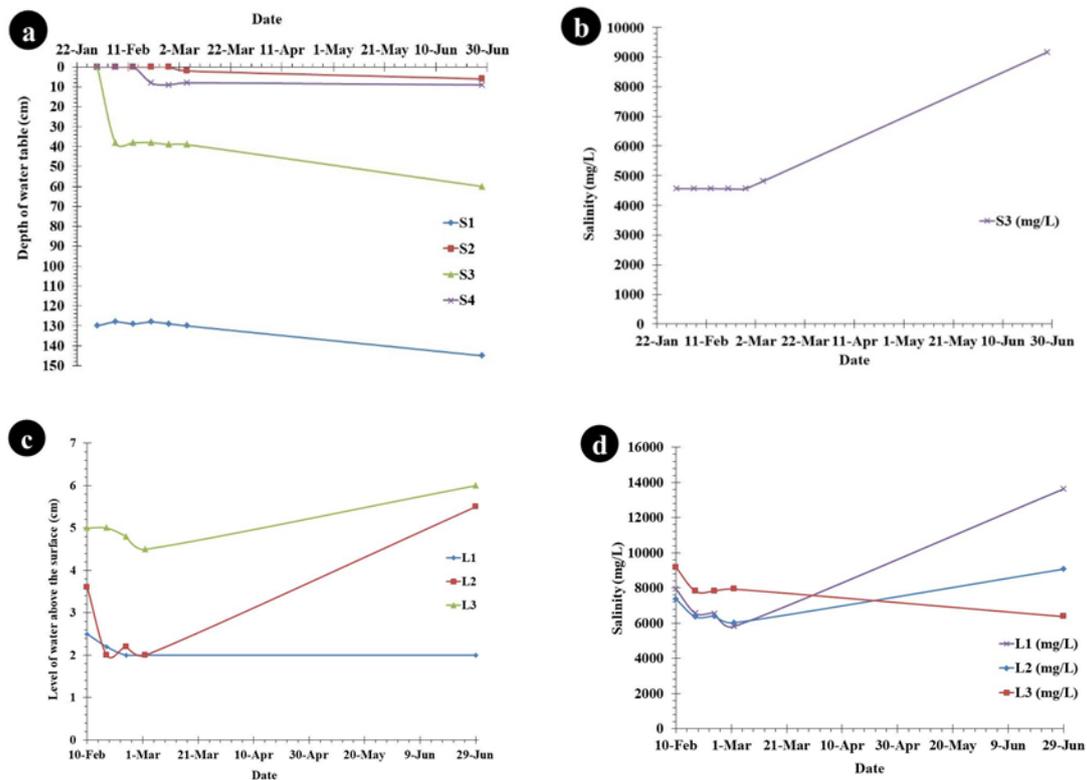


**Figure 4.** Field measurements. a) depth to water level in Wadi N, b) salinity of water in Wadi N, c) water level in Wadi M, d) salinity of water at surface in Wadi M.

the same salinity trend (ranging between 6,200 mg/L to 8,000 mg/L). After about 4 months (28<sup>th</sup>-June 2020), the salinity in L1 and L2 increased and reached 13,632 mg/L and 9,075, respectively, while it decreased in L3 to 6,374 mg/L. It was difficult to collect more information because of the lockdown due to the Covid-19 pandemic. However, it can be speculated that this behavior in salinity is due to excessive irrigation during summer. Infiltrated irrigation water may dissolve salts from the soil before seeping out into the wadi. It was not possible to get the information about the rate, volume and frequency of irrigation. The observed increase in ponded water levels in Wadi M can be attributed to the excessive fresh irrigation water applied to the trees around the wadi (Figure 8a and Figure 9d) as well as to seepage from the Botanic garden lake which is around 25 m away from wadi M (Figure 8b), and probably to leakages from the SQU water network (Figure 9c). The observed decrease in salinity during the period 10<sup>th</sup>-February to 2<sup>nd</sup>-March 2020 might be also caused by excessive irrigation and seepage from the lake. During the period 2<sup>nd</sup> of March to 28<sup>th</sup> June 2020, the water salinity at L3 continued to decrease. The shade of the canopy of large trees around the location presumably contributed in lowering the evaporation. On the other hand, the increase in water salinity for L1 and L2 may be due to the high evapora-

tion as these locations are less vegetated with absence of lower shading by the trees. It is noteworthy that the algal growth in the the wadi suggests that this water has been stagnant for a long time (Figure 8c, Figure 9a). Consequently, the ponded water in the wadi become smelly and a zone for breeding of insects. This may raise a risk to the health of residents of the campus, as well as increase the cost of application of insecticides and fumigation.

### Soil Heterogeneity

The alluvium soils of the study area were characterized by heterogeneous strata which is inherited from a parent material. The latter was formed by a complex lithostratigraphy having a mixed carbonate-siliciclastic sequence (Winterleitner et al., 2018). Soil profile lithologies and descriptions of wadi N revealed the soils of our site to have formed under intense diagenetic stratification, complex sedimentological events, and different geometry of geogenic depositions which ultimately resulted in such stratum heterogeneity (Figure 10a). The soil horizons of the wadi N soil profiles varied dramatically, even for some profiles being only a couple of meters apart. The variation of pedogenic and soil morphological features included: (i) the type and vertical heterogeneity in soil texture, (ii) distinctness and topography of the horizon boundaries, (iii) formation and stage of

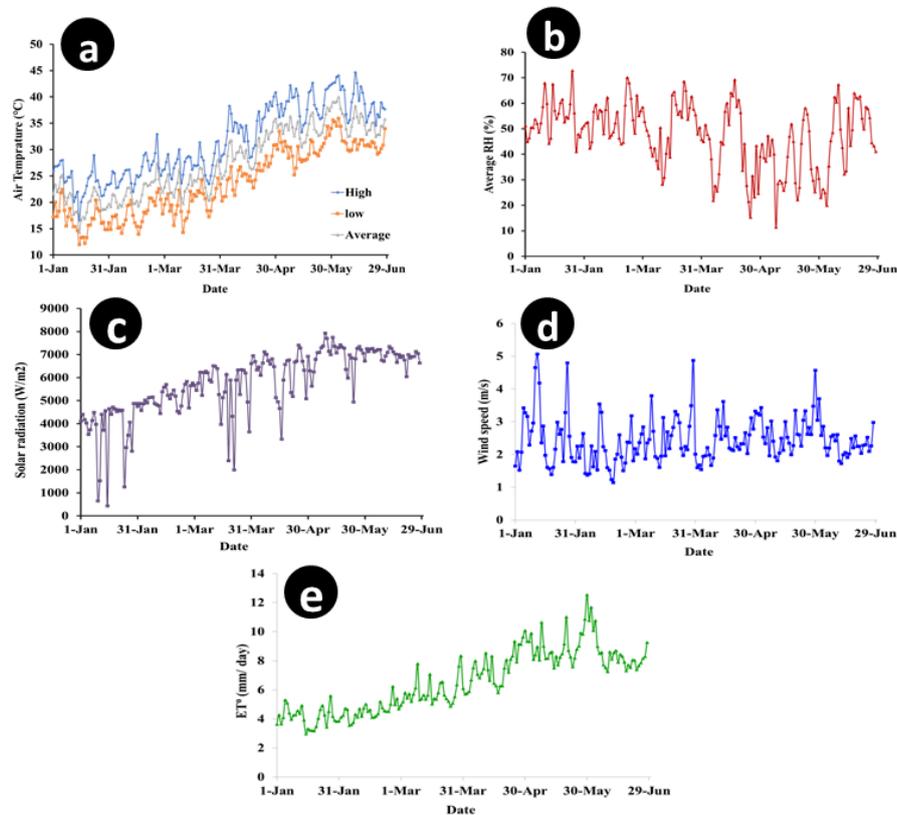


**Figure 5.** Daily average weather data. a) air temperature (°C), b) relative humidity (%), c) solar radiation (W/m<sup>2</sup>), d) wind speed (m/s<sup>2</sup>) e) reference evapotranspiration (mm/day).

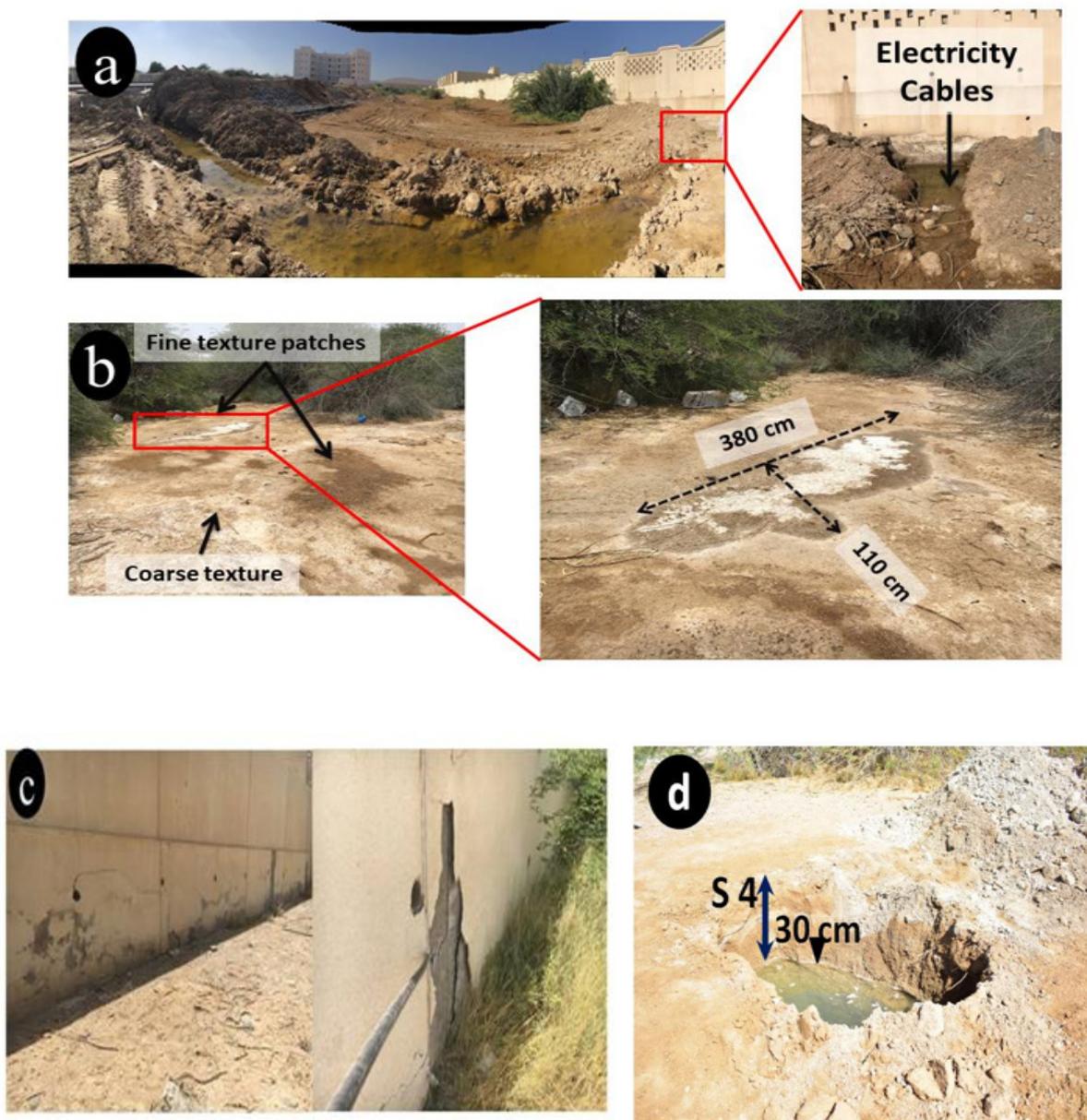


**Figure 6.** Field observation in Wadi N during February 2020. a) SWT in a construction site near S2 excavation , b) patched crystallized salt of fine texture, on the top of a coarse texture soil (zoomed in picture for the location indicated with the red-rectangle which is a fine texture patch with salt accumulation), c) cracking and paint peeling of walls due to shallow brackish water table, d) photo of S4 indicating the shallow water table

cementation of incipient and/or well developed caliche layers (Figure 10b), (iv) occurrence or absence of pebbles-cobbles-sized conglomerates (Figure 10c), (v) alternating sequence of silt/sandstones and conglomerates, (vi) formation of post-depositional altered silt and clay stone (Figure 10 d), and (vii) existence of tilted bedrock of limestone, among others.

### Water Chemistry

Groundwater samples were collected and analyzed immediately on the day of excavations. Table 3 is presenting the results of the groundwater quality analysis. Samples of crystalline salts at the surface were also collected along, with soil samples from all excavated pits, and the results are presented in Table 4.

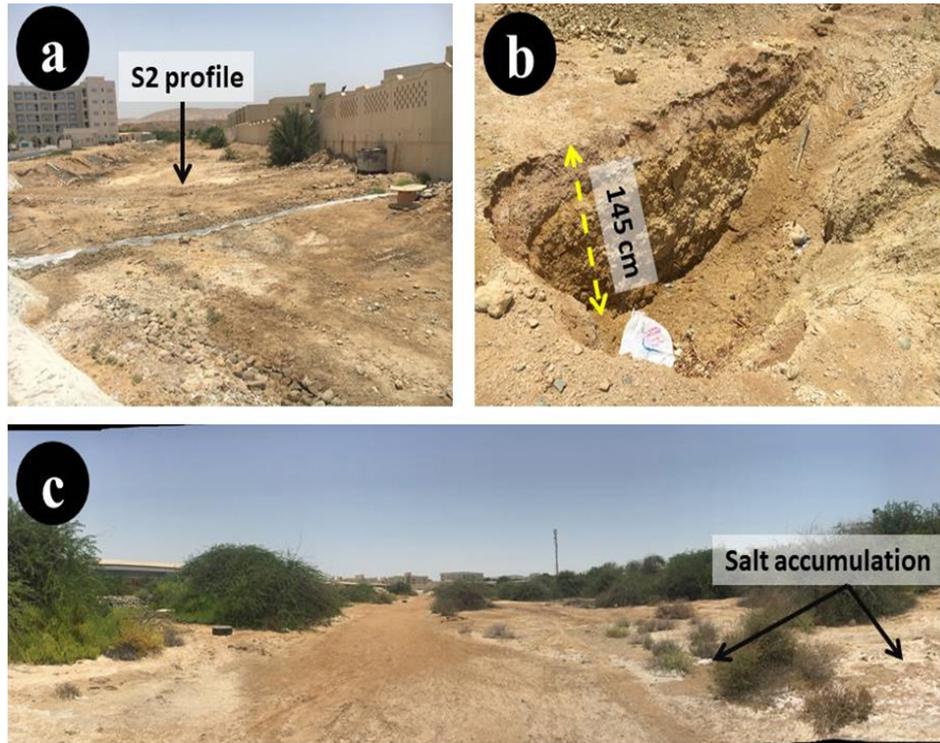


**Figure 7.** Field observation in Wadi N during June, 2020. a) area near S2 excavation, b) complete disappearance of water table in S1 excavation, c) salt accumulation near S3 and S4 excavations.

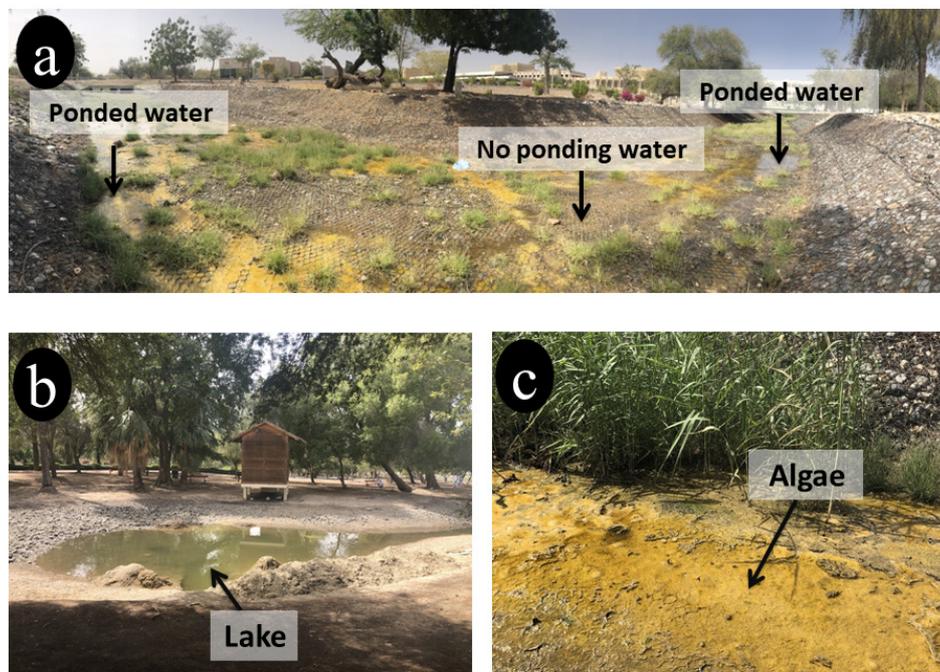


**Figure 8.** Field observation in Wadi M during February 2020. a) surface water distribution at Wadi M (23°35'20.07" N 58°09'49.88" E, elevation 53.6 m) between L1 and L2, b) Botanic garden lake near Wadi M (location 23°35'23" N, 58°09'56.46" E, elevation 51.2 m), c) ponded wadi water with algal growth.

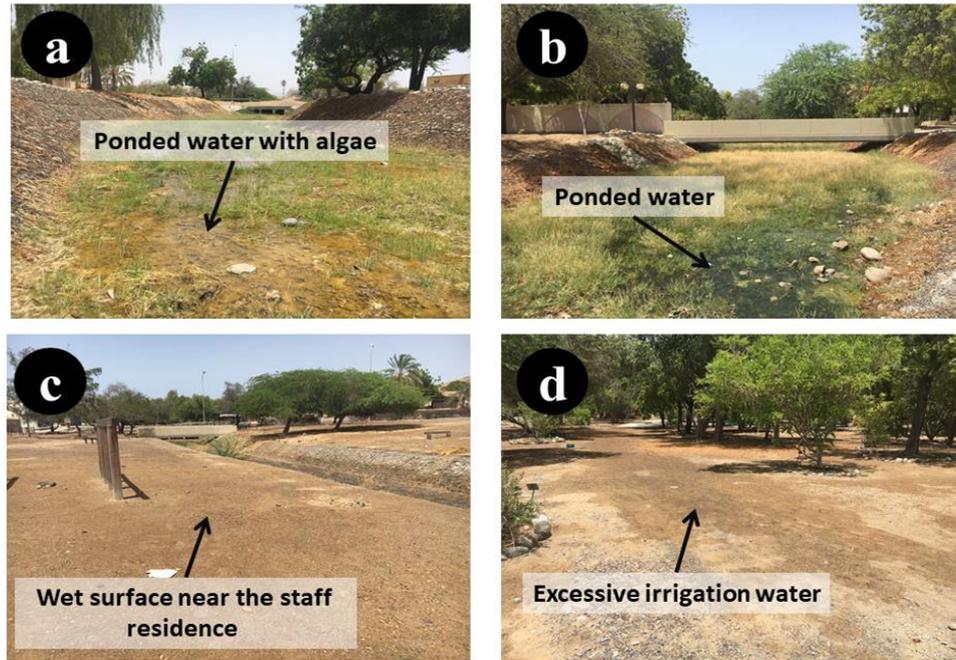


**Figure 9.** Field observation in Wadi M during June, 2020. a) surface water level with algae between L1 and L2, b) water level near L3, c) wet areas upstream, d) excessive irrigation of trees near the Wadi channel.

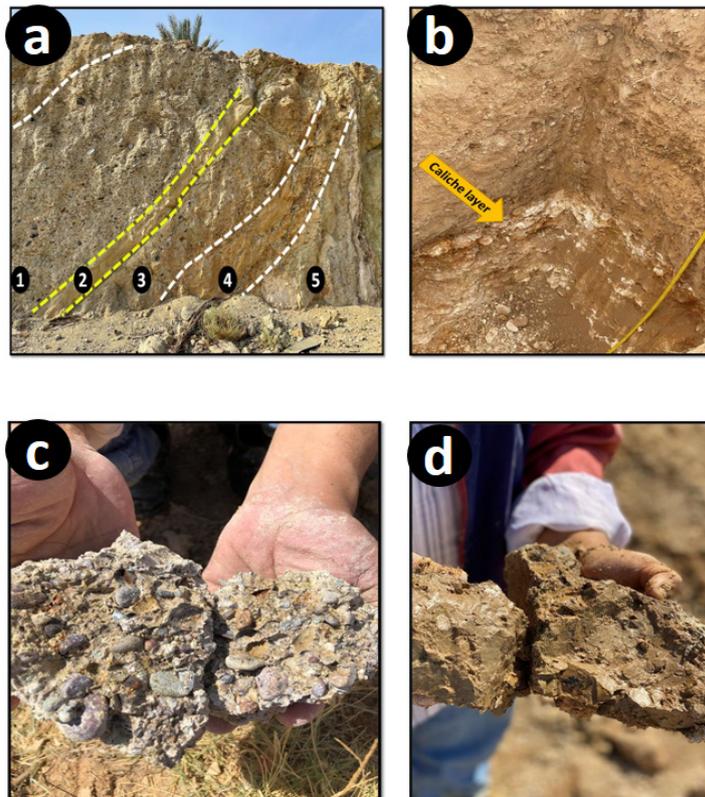


**Figure 10.** (a) Outcrop picture representing the complex soil lithology, sedimentology, and stratification of the study area. Note: the dash lines separate different layers that are indicated with numbers (b) Formation of a caliche layer in one of the soil profiles of Wadi N, (c) Chunks of pebbles-cobbles-sized conglomerates collected from studies soil profiles, (d) Blocks of post-depositional altered silt-clay-stone

**Table 3.** Analysis of the collected water samples from S3, S4 in Wadi N

S3		S4	
pH	7.9	pH	7.7
EC	11.68 mS/cm	EC	13.31 mS/cm
<b>Elements</b>	<b>Results in mg/L</b>	<b>Elements</b>	<b>Results in mg/L</b>
Al 396.152	-0.050342	Al 396.152	-0.150695
B 249.772	-0.017021	B 249.772	-0.006665
Ba 455.403	-0.098762	Ba 455.403	-0.09874
Be 313.042	-0.038596	Be 313.042	-0.038391
Ca 396.847	<b>568.263</b>	Ca 396.847	<b>635.63</b>
Cd 214.439	-0.032466	Cd 214.439	-0.030945
Co 238.892	-0.027427	Co 238.892	-0.02722
Cr 267.716	-0.025978	Cr 267.716	-0.028823
Cu 327.395	-0.019069	Cu 327.395	-0.050042
Fe 238.204	-0.01258	Fe 238.204	-0.088426
K 766.491	<b>25.652</b>	K 766.491	<b>31.2563</b>
Mg 279.553	<b>291.36</b>	Mg 279.553	<b>302.69</b>
Mn 257.610	-0.033855	Mn 257.610	-0.041611
Mo 202.032	-0.027972	Mo 202.032	-0.024372
Na 589.592	<b>1052.36</b>	Na 589.592	<b>1315.35</b>
Ni 231.604	-0.01236	Ni 231.604	-0.032289
P 213.618	-0.074991	P 213.618	-0.068768
Pb 220.353	-0.100803	Pb 220.353	-0.097095
Se 196.026	-0.055867	Se 196.026	-0.015623
Si 251.611	<b>14.9055</b>	Si 251.611	<b>12.017</b>
Sr 407.771	<b>7.17708</b>	Sr 407.771	<b>10.8295</b>
Ti 336.122	0.000255	Ti 336.122	0.000905
V 292.401	-0.043176	V 292.401	-0.050354
Zn 213.857	-0.04952	Zn 213.857	-0.048389

Both water and soil samples are rich of Ca, K, Na, and Mg. The geology of the area is a sedimentary tertiary limestone, which is rich of those minerals, and our hypotheses is that the perched water table is stable there for long time and groundwater is in chemical equilibrium with the minerals of the wadi bed sediments. This is substantiated by the water chemistry signature. Cycles of wetting and drying due to the infiltration events from the wadi bed and corresponding rises and drawdowns of the water table after rainfall events causes recirculation of salts in the shallow vadose zone above the water table. Repeated cycles of crystallization and dissolution of salts between the upper part of the soil/sediments and

the shallow water table take place. Detailed investigation of the isotopes are planned to be conducted in the future with indepth analysis of soil cores. A geophysical survey to delineate the dimensions and scales of this perched aquifer and the source of water are also planned.

#### HYDRUS-1D Simulation for WTR in S3

Figure 11 presents the evaporation rate for the HYDRUS-1D simulated scenarios. The daily evaporation rate for the period 1<sup>st</sup> to 28<sup>th</sup> –June 2020 (scenario 2) ranges from 0.57 to 0.93 cm/day. This is 1.46- 1.5 times higher than that for the period 31<sup>st</sup> - January to 5<sup>th</sup> – March 2020 (scenario 1) which ranges from 0.39-0.62

**Table 4.** Analysis of the collected crystalline salts from the soil surface near S4 in Wadi N.

SALT	
Elements	Results (mg/kg)
Al 396.152	-0.051616
B 249.772	-0.06055
Ba 455.403	-0.037573
Be 313.042	-0.100124
Ca 396.847	<b>10674.2</b>
Cd 214.439	-0.039942
Co 238.892	-0.034173
Cr 267.716	-0.032057
Cu 327.395	-0.037458
Fe 238.204	-0.034915
K 766.491	<b>940.5</b>
Mg 279.553	<b>87.5</b>
Mn 257.610	-0.014946
Mo 202.032	-0.053296
Na 589.592	<b>205111</b>
Ni 231.604	-0.042934
P 213.618	-0.025945
Pb 220.353	-0.073407
Se 196.026	-0.007935
Si 251.611	<b>26.704</b>
Sr 407.771	<b>95.25775</b>
Ti 336.122	0.000694
V 292.401	-0.072324
Zn 213.857	-0.072324

cm/day (Table 5). These results were realistic as it is expected to have a higher evaporation rate in June than in January-March due to higher air temperature (34.5-37.6 °C for June and 17.25-31.48 °C for January to March) (Figure 5a) and higher solar radiation. Based on these modeling results and the assumptions (flat area, homogeneous bare soil, evaporation was the only source of water loss), the total volume of evaporated water

from the whole area of Wadi N in the modeled period would be 6600 m<sup>3</sup> (Table 5). Moreover, these results are in agreement with the field observations, as the drop in the water table for S3 excavation was much higher for

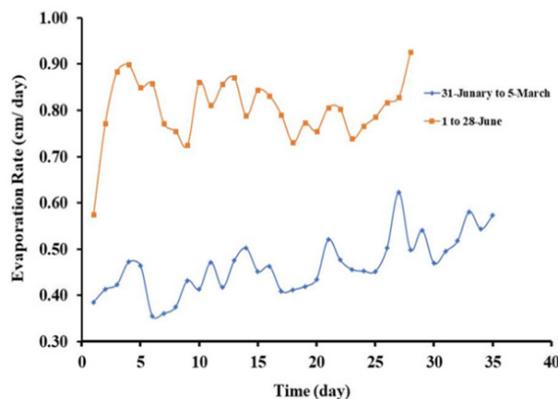


**Figure 11.** HYDRUS 1D simulated evaporation rate (cm/day) during the periods 31<sup>st</sup> January to 5<sup>th</sup> -March and 1 to 28- June 2020.

the period of 1<sup>st</sup> to 28<sup>th</sup> -June than 31<sup>st</sup> - January to 5<sup>th</sup> -March (Figure 4a). However, the reported modeling results have some uncertainties as they were based on observation from excavations and a soil profile of 1.5 m. The depth of the bed rock and the areal extension of the perched aquifer are still not known. From existing boreholes around SQU campus and nearby areas, it is known that the regional aquifer is around 20 m below the ground surface (Zlotnik et al., 2017).

Therefore, further studies should include detailed data about the lithology-sedimentology of the site. Core sampling with a fine vertical resolution from a network boreholes (to be drilled on SQU campus) is needed. A

**Table 5.** Summary result for calculation of evaporated water volume (m<sup>3</sup>) from Wadi N.

The parameter	Values
Average evaporation rate (31 <sup>st</sup> - January to 5 <sup>th</sup> -March 2020) (cm/day)	0.80
Average evaporation rate (1 <sup>st</sup> to 28 <sup>th</sup> -June 2020) (cm/day)	0.46
Difference in evaporation rate (cm/day)	0.34
No. days (31 <sup>st</sup> -January to 28 <sup>th</sup> -June 2020)	150
Difference in evaporation rate*No. days (cm)	50.70
Difference in evaporation rate*No. days (m)	0.51
Area of Wadi N (m <sup>2</sup> )	12941.25
Volume of evaporated water (m <sup>3</sup> )	6600

detailed geophysical study of the perched aquifer, vadose zone beneath it and of the regional aquifer is required. After acquiring these field data, HYDRUS and MODFLOW modeling can be carried out in a comprehensive study of water and solutes dynamics.

## Conclusion

The water table dynamics in Wadis N and M at SQU was studied for the period January to June, 2020. The main findings of this study are: the water table depth in Wadi N increased during June compared to the period January- March whereas the water level was above the bed surface in Wadi M where ponding increased continuously during the same period. The drop of water table in wadi N could be attributed to the effect of evaporation and discontinuity of the subsurface water source, as the source of water is, most probably, from the rainfall. For Wadi M, the increase of ponded water levels may be attributed to excessive irrigation in summer and possible leakage from the water network in the vicinity of the staff accommodation in the area. Crystallization and precipitation of salts on the soil surface increased over summer due to the high intensity of evaporation from the shallow water table in Wadi N and with absence of rainfall. Furthermore, based on numerical modeling of soil near S3 excavation in Wadi N, the evaporation rate for the period 1<sup>st</sup> to 28<sup>th</sup> -June 2020 was higher by 1.46-1.5 times than that for the period 31<sup>st</sup> - January to 5<sup>th</sup> -March 2020. This could be due to higher temperature and solar radiation in June, as compared to January and March. HYDRUS 1D-computed total volume of evaporated water from the entire area of Wadi N is 6600 m<sup>3</sup>. Further studies should include a geophysical survey to (i) determine groundwater quality, (ii) investigate underground pedogenic formations (especially the types of redox morphic features and the existence of low permeable caliche lenses that prevent vertical infiltration of water), and (iii) identify the nature, number, and type of aquifers in the study area, and locations for drilling the monitoring wells. A detailed water chemistry study and isotopic analysis are also needed. Additional HYDRUS modelling is required to assess different hydrological aspects in order to understand the dynamics of water in such SWT system. This will help in proposing the most appropriate solutions for coping with WTR at the site.

## Acknowledgement

Support of the Sultan Qaboos University through the internal grant (IG/VC/WRC/21/01) and the Research Group DR/RG/17 is highly acknowledged and appreciated. The technical help of Sultan Qaboos University and the Department of Soils, Water, and Agricultural Engineering is also appreciated. This work is part of the undergraduate student (the first author) research.

## References

- Abderrahman WA, Rasheeduddin M, Nejem JK. (2000). Impacts of irrigation on shallow groundwater in Eastern Province, Saudi Arabia. *International Journal of Water Resources Development* 16(3): 369-390.
- Abu-Rizaiza OS. (1999). Threats from groundwater table rise in urban areas in developing countries. *Water International* 24(1): 46-52.
- Abu-Rizaiza OS, Sarikaya HZ, Khan MA. (1989). Urban groundwater rise control: case study. *Journal of Irrigation and Drainage Engineering* 115(4): 588-607.
- Al Senafy M. (2011). Management of water table rise at Burgan oil field, Kuwait. *Emirates Journal of Engineering Research* 16(2): 27-38.
- Allocca V, Coda S, De Vita P, Iorio A, Viola R. (2016). Rising groundwater levels and impacts in urban and semirural areas around Naples (southern Italy). *Rendiconti Online Societa Geologica Italiana* 41: 14-17.
- Al-Mayahi A, Al-Ismaily S, Gibreel T, Kacimov A, Al-Maktoumi A. (2019). Home gardening in Muscat, Oman: Gardeners' practices, perceptions and motivations. *Urban Forestry & Urban Greening* 38: 286-294.
- Al-Sefry SA, Şen Z. (2006). Groundwater rise problem and risk evaluation in major cities of arid lands-Jeddah Case in Kingdom of Saudi Arabia. *Water Resources Management* 20(1): 91-108.
- Al-Senafy M, Hadi K, Fadlilmawla A, Al-Fahad K, Al-Khalid A, Bhandary H. (2015). Causes of groundwater rise at Al-Qurain residential area, Kuwait. *Procedia Environmental Sciences* 25: 4-10.
- Eberbach PL. (2003). The eco-hydrology of partly cleared, native ecosystems in southern Australia: a review. *Plant and Soil* 257(2): 357-369.
- Bob M, Rahman N, Elamin A, Taher S. (2016). Rising groundwater levels problem in urban areas: a case study from the Central Area of Madinah City, Saudi Arabia. *Arabian Journal for Science and Engineering* 41(4): 1461-1472.
- Kacimov A, Al-Maktoumi A, Šimůnek J. (2021). Water table rise in urban shallow aquifer with vertically-heterogeneous soils: Girinskii's potential revisited. *Hydrological Scienc* 66 (5): 795-808.
- Morway ED, Gates TK, Niswonger RG. (2013). Appraising options to reduce shallow groundwater tables and enhance flow conditions over regional scales in an irrigated alluvial aquifer system. *Journal of Hydrology* 495: 216-237.
- Radcliffe DE, Šimůnek J. (2018). *Soil physics with HYDRUS: Modeling and applications*. CRC Press, Boca Raton, FL.

- Raymond AJ, Tipton JR, Kendall A, DeJong JT. (2020). Review of impact categories and environmental indicators for life cycle assessment of geotechnical systems. *Journal of Industrial Ecology* 24: 485–499.
- Rufí-Salís M, Petit-Boix A, Villalba G, Sanjuan-Delmás D, Parada F, Ercilla-Montserrat M, Arcas-Pilz V, Muñoz-Liesa J, Rieradevall J, Gabarrell X. (2020). Recirculating water and nutrients in urban agriculture: An opportunity towards environmental sustainability and water use efficiency? *Journal of Cleaner Production* 261: Article 121213.
- Saeed F, Rahman M, Chamberlain D, Collins P. (2019). Asphalt surface damage due to combined action of water and dynamic loading. *Construction and Building Materials* 196: 530-538.
- Sharp JM. (2010). The impacts of urbanization on groundwater systems and recharge. *AQUA Mundi* 1(3): 51-56.
- Šimůnek J, Van Genuchten MT. (1999). Using the HYDRUS-1D and HYDRUS-2D codes for estimating unsaturated soil hydraulic and solute transport parameters. *Characterization and Measurement of the Hydraulic Properties of Unsaturated Porous Media* 1: 523-531.
- Šimůnek J, Van Genuchten MT, Šejna M. (2016). Recent developments and applications of the HYDRUS computer software packages. *Vadose Zone Journal* 15(7): 1-25.
- Soil Survey Staff. (2014). *Soil survey field and laboratory methods manual*. Soil Survey Investigations Report No. 51 Version 2. Lincoln, NE: USDA-NRCS.
- Van Genuchten, M. T. (1980). A closed-form equation for predicting the hydraulic conductivity of unsaturated soils. *Soil Science Society of America Journal* 44(5): 892-898.
- Winterleitner G, Schütz F, Wenzlaff C, Huenges E. (2018). The Impact of Reservoir Heterogeneities on High-Temperature Aquifer Thermal Energy Storage Systems. A Case Study from Northern Oman. *Geothermics* 74: 150-162.
- Zlotnik VA, Kacimov A, Al-Maktoumi A. (2017). Estimating groundwater mounding in sloping aquifers for managed aquifer recharge. *Groundwater* 55(6): 797-810.
- Zotarelli L, Dukes MD, Romero CC, Migliaccio KW, Morgan KT. (2010). *Step by step calculation of the Penman-Monteith Evapotranspiration (FAO-56 Method)*. Institute of Food and Agricultural Sciences. University of Florida, FL, US.